Desalination and Water Treatment
www.deswater.com
doi: 10.1080/19443994.2015.1030707

57 (2016) 9409–9419
April

Taylor & Francis
Taylor & Francis Group

Synthesis of titanate nanoparticles in low temperature hydrolysis and adsorption of arsenate (V) and fluoride

Hui Deng*, Kezheng Zhang, Xiaoning Wang

College of Chemistry, Chemical and Environment Engineering, Liaoning Shihua University, Fushun 113001, China, Tel. +86 24 56860759; email: dengchong9396@live.cn (H. Deng), Tel. +86 24 56860179; emails: zka@163.com (K. Zhang), wxn@163.com (X. Wang)

Received 31 August 2014; Accepted 6 March 2015

ABSTRACT

In this work, anatase titanium dioxide (TiO_2) with surface area (167 m^2/g) and pore size diameters (17.8 nm) was synthesized by low temperature one-step hydrolysis technique, and its adsorption abilities to arsenate and fluoride, the severe poisonous inorganic contamination in aqueous solution, were evaluated. TiO_2 prepared at hydrolysis temperature of 80°C and 0.2 mol/L $Ti(SO_4)_2$ concentration was optimum to remove As (V) and F^-. Batch experiments showed that the adsorption of As (V) was more favored in the range of pH 2.0–8.0, while the uptake of F^- was preferred only at pH 3.8. The maximum uptake calculated by Langmuir equation for As (V) and F^- was 49.28 mg/g (pH 5.0) and 32.15 mg/g (pH 3.8), respectively. Ionic strength hardly has any effect on As (V) and F^- removal. As (V) and F^- kinetics study indicated that both the adsorption processes occurred rapidly; more than 82.6% of As (V) and 78.5% of F^- could be adsorbed on TiO_2 in the first 100 min, but adsorption equilibrium was not obtained until 10 h. Interference studies on the effects of SO_4^{2-}, CO_3^{2-}, SiO_3^{2-}, and PO_4^{3-} illustrated that As (V) and F^- sorption were drastically influenced by PO_4^{3-}.

Keywords: Nanocrystalline TiO_2; Low temperature hydrolysis; Adsorption of arsenate and fluoride

1. Introduction

Arsenic is known to be a hazardous pollutant in ground and surface waters which can cause a variety of disease including arsenical dermatitis, heart disease, and cancer in the liver, lungs, skin, bladder, and kidneys [1]. Elevated arsenic concentration in aquatic environments is caused by natural processes such as dissolution of arsenic-containing minerals by weathering, and human activities such as use of arsenical pesticides [2]. Arsenic is predominantly present as As (III) and As (V) in the form of arsenite and arsenate, and the acceptable value of arsenic in drinking water is 10 μg/L according to the US Environmental Protection Agency and World Health Organization [3]. Arsenate (V) is the most stable surface water species under aerobic conditions and exists as deprotonated oxyanions of arsenic acid ($H_2AsO_4^{2-}$, $HAsO_4^{2-}$). Generally, As(III) remains undissociated and is neutral, and therefore exhibits only limited adsorption sites as compared to As (V) [4].

*Corresponding author.

Fluoride in drinking water may be beneficial or detrimental depending on its concentration and total amount consumed. For good health, the optimum fluoride level in drinking water should be in the range of 0.5–1.5 mg/L [5]. Concentration higher than this causes mottling of teeth in mild cases, even fluorosis (dental and/or skeletal) and several neurological damages in severe cases [6]. High fluoride levels in groundwater are worldwide problems; available statistics indicated that more than 300 million people are seriously affected by fluorosis [7].

Recently, nanoparticles are focused on application as sorbents for removal of pollutants due to their quite different physicochemical properties [8], such as the cupric oxide (CuO) nanoparticles [9], cellulose/HA [10], a binary mixed oxide of iron and silicon [11] nanocomposites, and iron(III) oxide-coated ethylenediamine-functionalized multiwall carbon nanotubes [12]. TiO_2 is effective in destroying a wide range of contaminants in gaseous and aqueous phases due to its physical and chemical stability, negligible toxicity, the resistance to corrosion, and strong oxidizing power of its holes and redox selectivity [13,14]. Titanium dioxide has been found to be a potential selective adsorbent for fluoride ions, as well as halogens and arsenic compounds [15,16]. The application of TiO_2 in arsenic removal can be divided into two aspects: TiO_2 functions as both photocatalyst and adsorbent in the presence of UV light or sunlight irradiation, but it works only as adsorbent in the absence of irradiation [17] The TiO_2 employed can be divided into several categories: nanocrystalline TiO_2 particles [18], titanate nanotubes [19], hydrous TiO_2 [20], granular TiO_2 [21], and TiO_2-impregnated chitosan beads [22].

As(III) has a lower affinity with mineral surfaces, while As (V) can be adsorbed easily into solid surface [23]. Therefore, the oxidation of As(III) to As (V) is necessary to be adsorbed onto metal oxyhydroxides [24]. The photocatalytic oxidation of As(III) to As (V) by TiO_2 is dependent on oxygen and the presence of light [25,26]. However, most of these studies have focused on the use of crystalline TiO_2 for As(III) catalytic oxidation followed by sorption [27]. Furthermore, numerous TiO_2 preparations were derived from solgel method [28,29], hydrolysis-precipitation method [30], precipitation [31], and microbial synthesis method [32]; limited studies have investigated synthesis of TiO_2 nanoparticles by low temperature hydrolysis.

The aim of this study was to develop and characterize a nanoscale titania-based sorbent for arsenate (V), and removal of fluoride from aqueous solution. The optimum preparation was explored, and the nature and morphology of nanocrystalline titania was characterized by SEM and XRD. Additionally, a series of batch adsorption experiments, including isotherm and kinetics studies, pH, and initial anions concentrations, were performed to better understand the adsorption behavior of the sorbent.

2. Materials and methods

2.1. Preparation of TiO_2 nanoparticles

Hydrolysis method: Different concentrations of titanium sulfate ($Ti(SO_4)_2$) aqueous solution were added into the reaction vessel, and the solution was heated at 80, 90, and 100°C for 5 h to produce the precipitate. The selection of an optimum temperature and $Ti(SO_4)_2$ concentration for TiO_2 sorbent was depends on the preparation method. After the hydrolysis, the mixture was filtered with DI water to neutral and the precipitate was desiccated at 100°C for 2 h.

2.2. Adsorbent characterization

X-ray powder diffractometer (XRD) analysis was carried out in D/max-IIIA powder diffractometer using Cu Kα radiation (λ = 1.5418 Å) at an scanning range of 2θ = 10–75° under a speed of 6°/min. The surface morphology (SEM) of the sorbent was analyzed using a scanning electron microscope (JEOL JSM-6301F). TEM analysis was measured by transmission electron microscope (JEOL JEM-2010). Surface area of the TiO_2 particles was measured by using Micrometrics (USA) BET (Brunauer, Emmett, and Teller) instrument using nitrogen intrusion technique. The microstructure of the sorbent was characterized using physical adsorption/desorption of nitrogen at −196°C. The samples were analyzed with an elemental analyzer, and on the basis of difference in the nitrogen content. Nitrogen isotherms are measured with an ASAP 2000 micropore analyzer at 77 K. The pH_{pzc} of TiO_2 was determined by the solid addition method [33].

2.3. Adsorption experiments

Batch experiments were performed to examine the adsorption behavior of arsenate and fluoride on TiO_2 nanoparticles. In experiments of TiO_2 preparation, the sorbent with a dose of 1 g/L was added into 100 mL of 100 mg/L As (V) and 10 mg/L fluoride, respectively, and the solution pH was adjusted by adding HCl and NaOH solution.

Adsorption of As (V) onto TiO_2 sorbents was first examined in a series of experiments where initial As (V) concentration was maintained constant for 5 mg L^{-1} by varying pH values (pH 2–11) and then

the optimum pH for adsorption was determined. Adsorption kinetics studies were conducted with 5 mg/L As (V) and the dose of TiO_2 was 10 mg at optimal pH. Adsorption isotherm experiments were carried out with the initial concentration of As (V) ranging from 1 to 200 mg/L at the optimal pH. All batch tests were performed in 250 mL glass flasks shaken at 125 rpm at 25°C for 24 h with 10 mg TiO_2 sorbent and 100 mL of As (V) solution. 0.5 M and 1 M $NaNO_3$ were used as electrolyte to analyze the effect of ironic strength. The initial and final As (V) concentrations in the solutions in each of the flasks were determined with an inductively coupled plasma emission spectrometer (ICP-ES, Thermo Electron, IRIS Intrepid, USA). Adsorption of fluoride was conducted in 250 mL plastic bottles in a similar way to As (V) adsorption; initial concentration of 10 mg/L fluoride solution was prepared with NaF. At the end of adsorption, the concentration of F^- in residual solution was analyzed by fluoride selective electrode determination. The competitive experiments were carried out in 5 mg/L As (V) solution at pH 6 and 10 mg/L F solution at pH 3.8, containing 0.1 or 1 mM Na_2SO_4, Na_2CO_3, Na_2SiO_3, and Na_3PO_4, respectively.

The amount of As (V) and F^- adsorption on the adsorbent at adsorption equilibrium, q_e (mg/g), was calculated from the equation;

$$q_e = V(C_0 - C_e)/m \quad (1)$$

where C_0 (mg/L) and C_e (mg/L) are the initial and final As (V) or F^- concentrations in the solution in each flask, respectively, V (L) is the volume of the solution in each flask, and m (g) is the weight of the adsorbent added into each flask.

3. Results and discussion

3.1. Adsorbent preparation

3.1.1. Hydrolysis temperature

In the preparation process, the hydrolysis of titanium sulfate and the temperature and station of solution may influence the performance of the resultant TiO_2 sorbent significantly. At the different hydrolysable temperatures, the agglomeration state, hydrolysis extent, and hydrate produced were probably different. Also the optimal hydrolyzable temperature was not same for the different titanium compounds. The higher the hydrolyzable temperature, the more drastic the hydrolysis process. Reaction temperature affected the reaction rate; the reaction at a high temperature shortened the nucleation, growth, and crystallization time [34], while quick generation of TiO_2 precipitation would obstruct $Ti(SO_4)_2$ hydrolysis, and led to a decrease in TiO_2 yield. The boiling point of water was 100°C and it was the highest limit to be obtained by low temperature hydrolysis. On the other hand, the hydrolysis rate was too slow to be adopted for practice if the hydrolyzable temperature was below 80°C. The As (V) and F^- removal results with these TiO_2 sorbents for 24 h adsorbing experiment are shown in Fig. 1.

It can be seen that the adsorption efficiency was minimum at 100°C, so the mild and slow hydrolysis process was favored for TiO_2 sorbent performance. For the economic reason, the hydrolyzable temperature of 80°C was adopted in the present study.

3.1.2. Titanium sulfate concentration

The adsorbed amounts of As (V) and F^- using the TiO_2 sorbents prepared from the different initial concentrations of $Ti(SO_4)_2$ solution are illustrated in Fig. 2. As shown in Fig. 2, the initial concentration of $Ti(SO_4)_2$ had a profound impact on As (V) and F^- adsorption. The maximum adsorption capacity was obtained when $Ti(SO_4)_2$ solution was 0.2 mol/L both for As (V) and F^-. TiO_2 production attributed to crystalline formation during hydrolysis procedure; a large number of nuclei were formed when the initial reaction solution was supersaturated, the growth group moved and adsorbed on nuclei surface, and grew into the crystalline phase at a suitable position. The crystalline gradients became regular with an increase in crystallization time, and small grains were translated

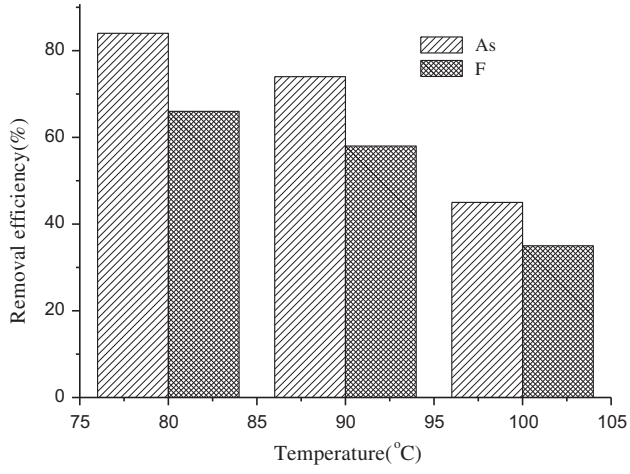

Fig. 1. Effect of hydrolysis temperature on nanocrystalline TiO_2 performance for As (V) and F removal (0.2 mol/L Ti $(SO_4)_2$, 100 mg/L As (V), and 10 mg/L F^-).

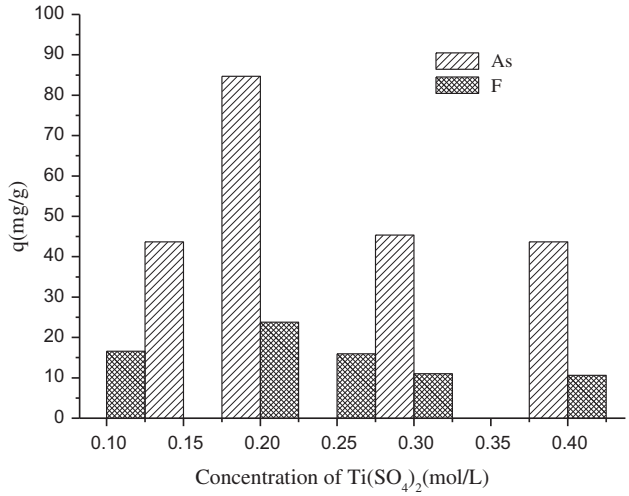

Fig. 2. Effect of initial $Ti(SO_4)_2$ concentration on nanocrystalline TiO_2 performance for As (V) and F^- removal (80°C hydrolysis temperature, 100 mg/L As (V) and 10 mg/L F^-).

into big crystal grains and made the average grain size increase with the desorption of growth group from crystalline phase [35]. Surface defects became few and reaction activity decreased after the grain size grew, so the increasing speed of grain slowed, and the synthesized speed of TiO_2 slowed.

3.2. Characterization of nanocrystalline TiO_2 sorbent

TiO_2 synthesized by hydrolysis method had well-defined and uniform particle morphology as presented in Fig. 3. From SEM photo shown in Fig. 3(a), individual particle sizes can be conclusively seen, and the difference between single particles or aggregates can be distinguished. The tiny particles aggregated into some bigger pellets, and there were plenty of micropores but only few macropores. TEM photo of Fig. 3(b) illustrated that the microcrystallites exhibited regular polygon, with sizes about 20 nm. In Table 1, it is shown that the particles of TiO_2 were much smaller than 20 nm according to the Scherrer equation.

XRD pattern of TiO_2 adsorbents in Fig. 4 suggested that the synthesized product was anatase. As reported by other researchers, the presence of peaks as an attributive indicator of anatase titania (2θ = 25.8, 37.80, 48.05) [36] was detected. Additionally, the specific surface area of the prepared Ti-based sorbents using the BET measurement was 167 m^2/g, and the pH_{PZC} of TiO_2 adsorbent was about 6.8, approaching the previous research [37].

3.3. Adsorption studies

3.3.1. pH effects

As (V) and F^- removal dependent on solution pH are illustrated in Fig. 5. The adsorption of As (V) remained stable during pH 2.0–8.0 but rapidly decreased when pH increased from 8 to 11. F^- uptake decreased with an increase in pH i.e 3.8. Both the maximum sorption amount of arsenate and fluoride occurred at $pH < pH_{pzc}$, since the TiO_2 sorbent surface was positive and suitable to attract the negative As (V) and F^-.

These results could be interpreted with regard to the solubility of hydrous titanium. According to the equilibrium calculation of solubility, the formation of $Ti(OH)_2^{2+}$ and $Ti(OH)^{3+}$ occurred at pH ≤ 2, the neutral species $Ti(OH)_4$ (aqueous) coexisted with $Ti(OH)_2^{2+}$ and $Ti(OH)^{3+}$ at about pH 3, and $Ti(OH)_4$ (aqueous) was formed dominantly by hydrolysis of Ti(IV) in the

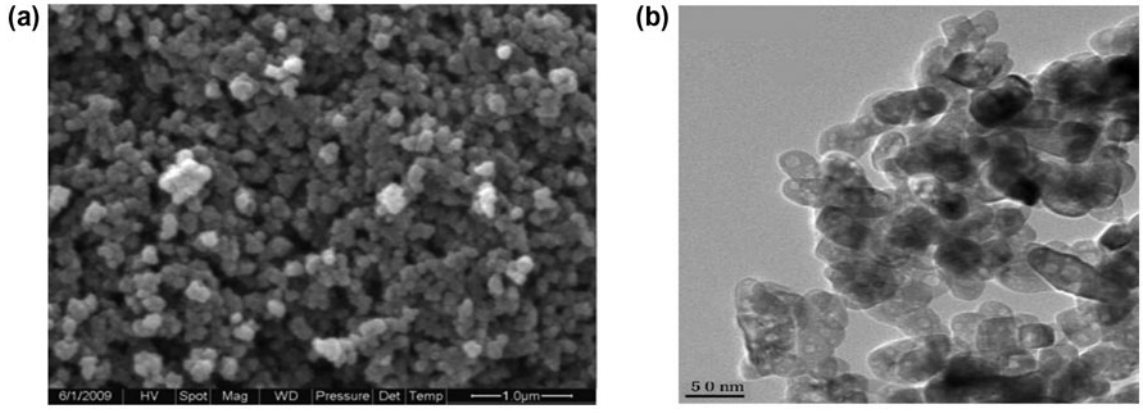

Fig. 3. The SEM image (a) and TEM photo (b) of nanocrystalline TiO_2 adsorbent (80°C hydrolysis temperature and 0.2 mol/L $Ti(SO_4)_2$).

Table 1
Physicochemical properties of the studied TiO_2 adsorbent. (80℃ hydrolysis temperature and 0.2 mol/L $Ti(SO_4)_2$)

Property	Value
Crystal form	Anatase
BET specific surface area[a]	167 m^2/g
Crystallite size[b]	17.8 nm
pH_{PZC}[c]	6.8

[a]By Micrometrics ASAP 2020 surface area and porosity analyzer with N_2 as the adsorptive gas.
[b]Calculated from XRD data.
[c]By the solid addition method [33].

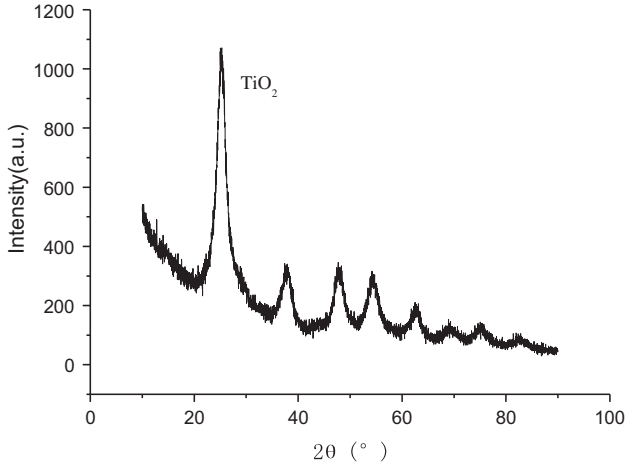

Fig. 4. The XRD pattern of the nanocrystalline TiO_2 adsorbents (80℃ hydrolysis temperature and 0.2 mol/L Ti $(SO_4)_2$).

region of $4 \le pH \le 10$ [31]. $Ti(OH)^{3+}$ (aqueous) was a metastable species with active adsorption characteristics of anatase and fluoride ion. So reduction of fluoride sorption at $pH > 3.8$ can be explained by the species change from $Ti(OH)^{3+}$ to $Ti(OH)_4$ (aqueous). In addition, HF was weakly ionized (pKa = 3.2) in solution at low pH values, and F^- was the major species at $pH > 3.2$. $H_2AsO_4^-$ was predominant species in a range of pH 2.26–6.67, while $HAsO_4^{2-}$ became major species at pH above 6.67 [38]. Therefore, uptakes of As (V) or F reduced since repulsive forces between As (V) or F^- ions and TiO_2 sorbent surface strengthened with an increasing pH value. The strong adsorption of arsenate at $pH > pH_{PZC}$ might suggest that the arsenic species were adsorbed on TiO_2 through surface complexation, rather than electrostatic interactions. Simultaneously, an increasing amount of hydroxyl ions in solution competed the adsorption sites with arsenate and fluoride with an increase in pH value.

3.3.2. Adsorption kinetics

Kinetic experiments were performed to determine the sorption rate of As (V) and F^- onto the sorbents as shown in Fig. 6. The sorption was particularly fast and most of the As (V) and F^- adsorbed in the first 100 min, but longer contact time was demanded for the effective uptake of arsenate on TiO_2 compared to fluoride. The equilibrium time required of fluoride on TiO_2 was found to be 6 h, while arsenate sorption equilibrium achieved after 10 h.

The kinetics results obtained from batch experiments were analyzed using different kinetics models

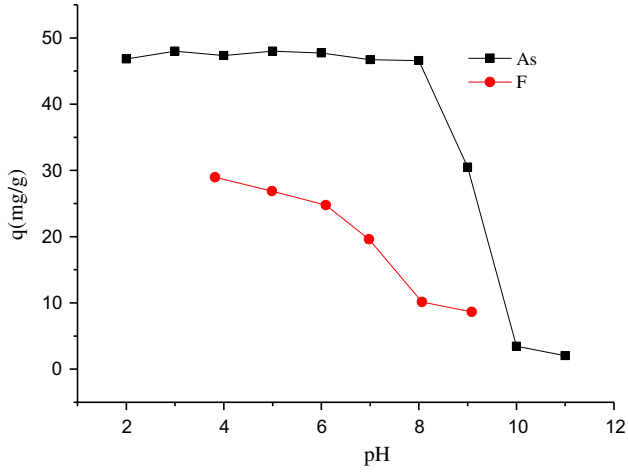

Fig. 5. Effect of solution pH on the adsorption of As (V) and F^- onto anatase TiO_2 (5 mg/L As (V) and 10 mg/L F^-).

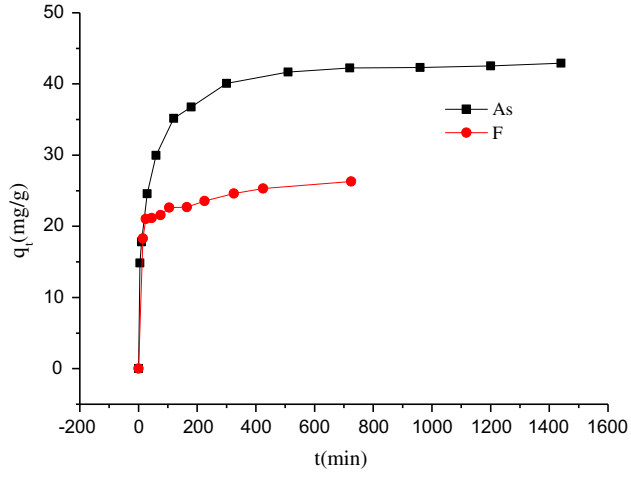

Fig. 6. Adsorption kinetics of As (V) and F^- on nanocrystalline TiO_2 (5 mg/L As (V) pH 6.0 and 10 mg/L F^- pH 3.8).

such as Lagergren pseudo-first-order [39,40], pseudo-second-order [41,42], and particle diffusion [43,44] models respectively.

The pseudo-first-order model:

$$\log (q_e - q_t) = \log q_e - k_1 t/2.303 \quad (2)$$

The pseudo-second-order model:

$$t/q_t = 1/k_2 q_e^2 + t/q_e \quad (3)$$

The intraparticle diffusion model:

$$q_t = 1/k_i t^{0.5} \quad (4)$$

where q_t (mg/g) was the uptake of As (V) or F^- at time t, q_e (mg/g) was the sorption capacity at equilibrium; and k_1 (min^{-1}) was the Lagergren pseudo-first-order rate constant in sorption process, k_2 (mg/g min) was the rate constant in the pseudo-second-order sorption process, k_i (mg/g $min^{0.5}$) was the intraparticle diffusion rate constant. The values of k_1, k_2, k_i, and the regression coefficients evaluated from the linear portions are presented in Table 2.

Goodness of fitness of the linear plot of these kinetic models can be judged from the value of the coefficient of the plot, which can also be regarded as the criterion in the determination of adequacy of a kinetic model. As shown in Table 2, the coefficients of As (V) and F^- were 0.9998 and 0.9984 respectively, and then the adsorption on nanocrystalline TiO_2 sorbent was regarded as pseudo-second-order rather than Lagergren pseudo-first-order and intra-particle diffusion models.

3.3.3. Effect of initial concentration

Impacts of initial concentration of As (V) and F^- on TiO_2 adsorption were assessed in Fig. 7. It was found that the sorption amount increased with increasing equilibrium arsenate or fluoride concentrations. The sorption capacity of As (V) was 43.87 mg/g at the equilibrium concentration of 35.83 mg/L. The sorption amount reached the equilibrium after the fluoride equilibrium concentration was 35 mg/L, and the respective sorption capacity was 31.8 mg/g.

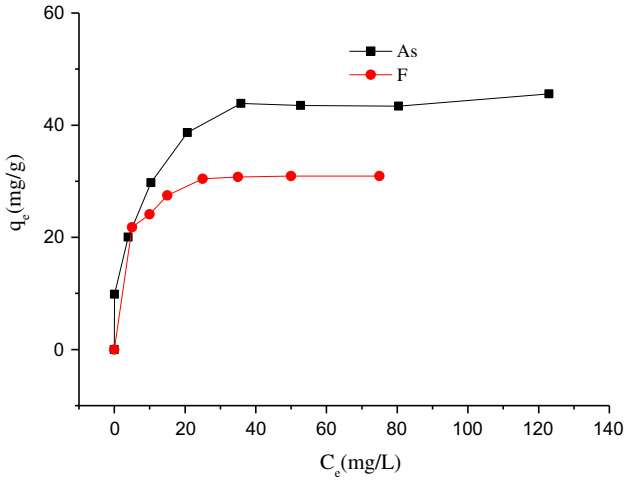

Fig. 7. Effect of initial concentration of As (V) and F^- on nanocrystalline TiO_2 (5 mg/L As (V) pH 6.0 and 10 mg/L F^- pH 3.8).

Langmuir and Freundlich isotherm equations were used to describe the experimental data in order to determine the adsorption capacity. Results using these two isotherms to fit the experimental data are presented in Table 3. Langmuir model assumed that adsorption forces were similar to the forces in chemical interaction, and valid for monolayer sorption onto a surface was described as [45]:

$$q_e = bQ_0C_e/(1 + bC_e) \quad (5)$$

where C_e was equilibrium concentration (mg/L), q_e was the amount adsorbed under equilibrium (mg/g), Q_0 was the theoretical maximum adsorption capacity,

Table 2
Adsorption kinetics parameters of nanocrystalline TiO_2 to As (V) and F^-

Dynamic equations	Anion	Dynamic parameters	Correlations coefficient R^2
Pseudo-first-order equation: $\log (q_e - q_t) = \log q_t - k_1 t$	As (V)	$k_1 \times 10^3 = 1.15$	0.7101
	F^-	$k_1 \times 10^3 = 1.38$	0.7271
Pseudo-second-order equation: $t/q_t = 1/k_2 q_e^2 + t/q_e$	As (V)	$k_2 \times 10^3 = 1.02$	0.9998
	F^-	$k_2 \times 10^3 = 2.58$	0.9984
Particle diffusion equation: $q_t = k_t t^{1/2}$	As (V)	$k_t = 12.6$	0.9266
	F^-	$k_t = 12.52$	0.8426

Table 3
Langmuir parameters of As (V) and fluoride adsorbed on TiO_2

	Langmuir model			Freundlich model		
Anion	b (L/mg)	q_m (mg/g)	R^2	k_F	n	R^2
As (V)	0.2821	49.28	0.9999	49.34	7.837	0.8783
F	0.4289	32.15	0.9992	18.03	7.1225	0.8761

and b (L/mg) was a Langmuir constant which indicated the affinity of the F^- and As (V) towards the adsorbent.

The Freundlich adsorption isotherm was based on the multilayer adsorption of an adsorbate onto the heterogeneous adsorbent surface, and could be expressed as [46]

$$q_e = k_F C_e^{1/n} \quad (6)$$

where K_F and $1/n$ were Freundlich constants, related to adsorption capacity and adsorption intensity (heterogeneity factor), respectively. The values of K_F and $1/n$ were obtained from the slope and intercept of the liner Freundlich plot of log q_e versus log C_e. The values of $1/n$ lying between 0 and 1 confirmed the favorable conditions for adsorption.

As seen from Table 3, Langmuir isotherm had high correlation coefficients R values than Freundlich isotherm, which indicated that the Langmuir isotherm described well for the sorption of As (V) and F^- on the nanocrystalline TiO_2 sorbent. A maximum adsorption calculated from Langmuir equation was used as the adsorption capacity. The adsorption capacities calculated are 49.28 mg/g for As (V) and 32.15 mg/g for F^-, respectively. The maximum sorption amount of fluoride calculated from Langmuir equation was close to that determined in actual measurements (31.8 mg/g), which suggested TiO_2 sorbent was almost saturated over the entire initial fluoride concentration range (5–100 mg/L). But there were free adsorption sites on TiO_2 nanoparticles to be occupied for As (V), and obviously TiO_2 sorbent had a stronger affinity to As (V) than fluoride.

Table 4 listed the sorption capacity of some sorbents reported in literatures. Ferric hydroxide was the most commonly used adsorbent in actual application for arsenic removal, but its sorption capacity for As (V) was not satisfactory. Zirconium-based sorbents

Table 4
Comparison of adsorption capacity of As (V) on different adsorbent

Adsorbent	Adsorption capacity (mg/g)	As (V) concentration (mg/L)	pH	References
Zirconium nanoparticle sorbent	39.06	5	2.5–3.5	[47]
Monoclinic hydrous zirconium oxide (ZR resin)	89.90	75	4–6	[48]
Aminated fibers	1.7	0.01	7.0	[38]
Activated alumina	8.8	1	7.2	[49]
Ferric hydroxide	1.1	0.01	6.5	[50]
Goethite	0.482	5.02	6.0	[51]
Ferric-impregnated volcanic ash	5.3008	5–100	6.9	[52]
Ceramic adsorbent	4.1851	5–100	6.9	[53]
Titanium dioxide-loaded Amberlite XAD-7 resin	4.72	0–375	1–5	[54]
Nanocrystalline titanium dioxide	11.2	0.15	7.0	[55]
Titanium dioxide suspensions	22.5	74.8	4.0	[56]
Hydrous titanium dioxide	33.4	1	4.0	[57]
Granular titanium dioxide	41.4	0.3	7.0	[58]
Fe–Mn binary oxide	63.8	1.9	5.0	[59]
Ce–Ti oxide sorbent	7.5	0.01	6.5	[60]
Nanocrystalline TiO_2	42.9	5	6.0	This study

Table 5
Comparison of adsorption capacity of F^- on different adsorbent

Adsorbent	Adsorption capacity (mg/g)	F^- concentration (mg/L)	pH	References
Lanthanum hydroxide	242.2	10–150	2.6	[61]
KMnO4-modified carbon	15.9	5–20	2.0	[62]
Activated alumina	2.41	2.5–14	7.0	[63]
Ferric Hydroxide	3	1	6.0–7.0	[64]
Titanium hydroxide-derived adsorbent	55.1	50	3.0	[54]
Nd-modified chitosan	22.38	10–100	7.0	[43]
Goethite	0.315	10.2	6.0	[51]
Aluminum and iron oxides	2.3	10	7.0	[65]
Titanium-rich bauxites	1.2	1	6.0	[66]
Fe–Ti oxide nano-adsorbent	47.0	50	–	[67]
Ti–Ce hybrid oxides	9.6	1	3–9.5	[68]
Ti–La hybrid oxides	15.1	1.7	3–9.5	[68]
Nanocrystalline TiO_2	32.15	10	4.0	This study

including zirconium nanoparticle sorbent and ZR resin had higher sorption capacity for As (V). Although the sorption capacities of As (V) on the reported adsorbents were obtained at different solution pH and equilibrium concentrations, it has been observed that the nanocrystalline TiO_2 in this paper was more powerful in efficiency.

Table 5 listed the sorption capacity of fluoride on the different adsorbents reported in the literature. Activated alumina was the most widely used sorbent in actual fluoride removal, but its adsorption capacity was so low as 2.41 mg/g. Recently, it was reported that the hydrous oxides of rare earth elements such as La(III), Ce(IV), and Zr(IV) have high sorption capacity for fluoride [69]. As shown in Table 5, the Lanthanum hydroxide had a high F^- sorption capacity about 242.2 mg/g, and titanium-based binary metal oxide sorbents such as Ti–Ce, Ti–La hybrid oxides had good adsorption ability for fluoride. It was seen that TiO_2 sorbent can be effectively used for removal of fluoride from aqueous solutions.

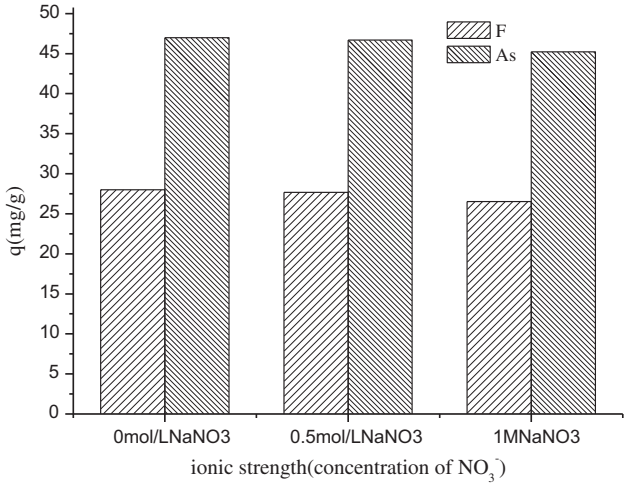

Fig. 8. The effect of ionic strength on adsorption capacity of As (V) and F (5 mg/L As (V) pH 6.0 and 10 mg/L F^- pH 3.8).

3.3.4. Ionic strength

Using $NaNO_3$ as background electrolyte, the effect of electrolyte on the As (V) and F^- adsorption on TiO_2 sorbent is shown in Fig. 8 compared with the results without electrolyte. No evidently competitive effects of NO_3^- were found on adsorption of As (V) and F^- in electrolyte solution though it was expected that the presence of anions in solution would enhance coulomb repulsion forces between anions and fluoride or would compete with fluoride for the active sites [70]. As (V) and F^- existed as a positive monovalent ion, benefit for adsorption at the pH values was considered ($pH < pK_{PZC} = 6.8$). It would be deduced that As (V) and F^- uptake by TiO_2 sites resulted from ion-exchange and inner-sphere surface complexation from notion of Fuhrman [71] and the weak dependence of the uptake on ionic strength was due to the formation of inner sphere complexes by the target sorbate.

3.3.5. Effect of competitive ions

Effects of common ions (phosphate, bicarbonate, silicate, and sulfate) in adsorption of As and F by TiO_2 are shown in Fig. 9(a) and (b), respectively. It can be seen that these anions at different concentrations

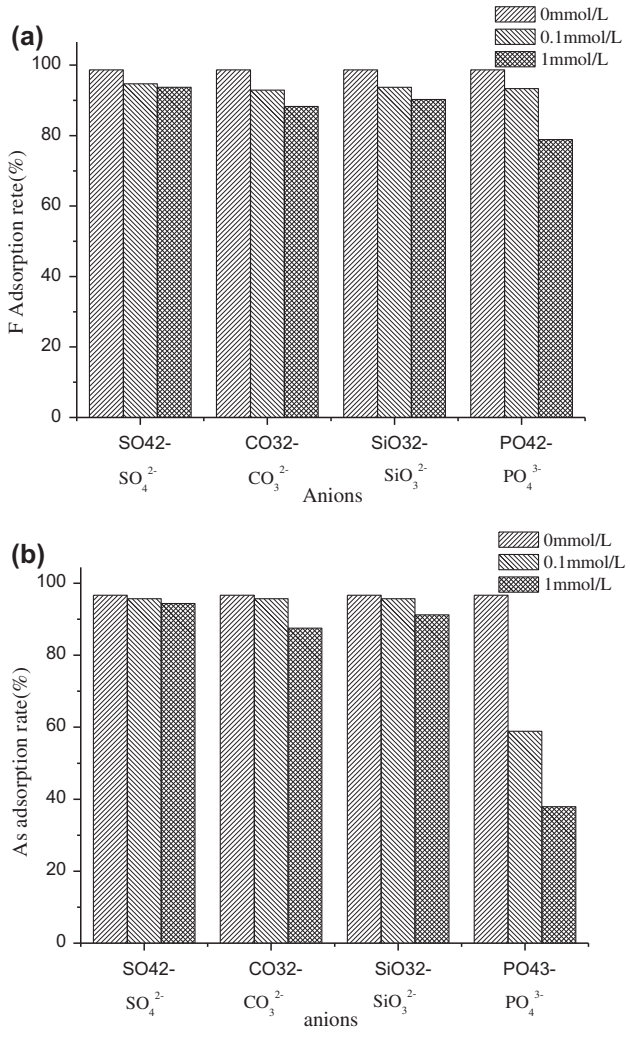

Fig. 9. Effects of competitive anions on F (a) and As (V) (b) removal by the TiO_2 sorbent.

(0.1 mM and 1 mM) had different effects on the sorption of F and As (V). Among these anions, PO_4^{3-} leads to the greatest decrease in F and As (V) adsorption. In addition, PO_4^{3-} caused a severe drop of As (V) than that for F, which attributed to similar ionization constants and ionic structure of PO_4^{3-} and As (V) [72]. SO_4^{2-} has little influence on F or As (V) sorption by TiO_2 sorbent, and adsorption rates of both F and As (V) followed the decreasing order of $PO_4^{3-} > CO_3^{2-} > SiO_3^{2-} > SO_4^{2-}$.

4. Conclusion

The TiO_2 nanocrystalline was prepared through hydrolysis at low temperature (80°C) with high surface area; uniform particle sizes have exhibited fast uptake rate and high adsorption capacity for As (V) and F^-. The optimum solution pH values for As (V) and F^- were obtained at $pH < pH_{PZC}$. Kinetics plots confirmed applicability of pseudo-second-order model expression for adsorption of As (V) and fluoride on TiO_2 sorbent. The Langmuir isotherm equation could be well used to describe the adsorption of As (V) and fluoride adsorption. As (V) and F^- uptake by TiO_2 sites was possibly due to ion-exchange and inner-sphere surface complexation. Comparison studies indicated that titanate materials exhibited great adsorption capacity to arsenate and fluoride; much higher than that for many reported adsorbents.

References

[1] J.C. Ng, J. Wang, A. Shraim, A global health problem caused by arsenic from natural sources, Chemosphere 52 (2003) 1353–1359.
[2] S. Kleinert, E.M. Muehe, N.R. Posth, U. Dippon, B. Daus, A. Kappler, Biogenic Fe(III) minerals lower the efficiency of iron-mineral-based commercial filter systems for arsenic removal, Environ. Sci. Technol. 45 (2011) 7533–7541.
[3] M. Berg, S. Luzi, P.T.K. Trang, P.H. Viet, W. Giger, D. Stüben, Arsenic removal from groundwater by household sand filters: Comparative field study, model calculations, and health benefits, Environ. Sci. Technol. 40 (2006) 5567–5573.
[4] T. Mahmood, S.U. Din, A. Naeem, S. Tasleem, A. Alum, S. Mustafa, Kinetics, equilibrium and thermodynamics studies of arsenate adsorption from aqueous solutions onto iron hydroxide, J. Ind. Eng. Chem. 20 (2014) 3234–3242.
[5] K. Babaeivelni, A.P. Khodadoust, Adsorption of fluoride onto crystalline titanium dioxide: Effect of pH, ionic strength, and co-existing ions, J. Colloid Interface Sci. 394 (2013) 419–427.
[6] N. Chen, Z.Y. Zhang, C.P. Feng, N. Sugiura, M. Li, R.Z. Chen, Fluoride removal from water by granular ceramic adsorption, J. Colloid Interface Sci. 348 (2010) 579–584.
[7] C. Reimann, K. Bjorvatn, B. Frengstad, Z. Melaku, R. Tekle-Haimanot, U. Siewers, Drinking water quality in the Ethiopian section of the East African Rift Valley I —Data and health aspects, Sci. Total Environ. 311 (2003) 65–80.
[8] G. Horányi, E. Kálmán, Anion specific adsorption on Fe_2O_3 and AlOOH nanoparticles in aqueous solutions: Comparison with hematite and γ-Al_2O_3, J. Colloid Interface Sci. 269 (2004) 315–319.
[9] K.J. Reddy, K.J. McDonald, H. King, A novel arsenic removal process for water using cupric oxide nanoparticles, J. Colloid Interface Sci. 397 (2013) 96–102.
[10] X.L. Yu, S.R. Tong, M.F. Ge, J.C. Zuo, Removal of fluoride from drinking water by cellulose@hydroxyapatite nanocomposites, Carbohydr. Polym. 92 (2013) 269–275.
[11] T. Mahmood, S.U. Din, A. Naeem, S. Mustafa, M. Waseem, M. Hamayun, Adsorption of arsenate from aqueous solution on binary mixed oxide of iron and silicon, Chem. Eng. J. 192 (2012) 90–98.

[12] Z. Veličković, G.D. Vuković, A.D. Marinković, M.S. Moldovan, A.A. Perić-Grujić, P.S. Uskoković, M.Đ. Ristić, Adsorption of arsenate on iron(III) oxide coated ethylenediamine functionalized multiwall carbon nanotubes, Chem. Eng. J. 181–182 (2012) 174–181.
[13] D. Nabi, I. Aslam, I.A. Qazi, Evaluation of the adsorption potential of titanium dioxide nanoparticles for arsenic removal, J. Environ. Sci. China 21 (2009) 402–408.
[14] T. Balaji, H. Matsunaga, Adsorption characteristics of As(III) and As(V) with titanium dioxide loaded amberlite XAD-7 resin, Anal. Sci. 18 (2002) 1345–1349.
[15] M. Tsuji, M. Abe, Possible radiochemical separations of anionic radionuclides by amorphous hydrous titanium dioxide, J. Radioanal. Nucl. Chem. Art. 102 (1986) 283–294.
[16] M. Tsuji, M. Abe, Selective uptake of toxic elements by an amorphous titanium dioxide ion exchanger, J. Radioanal. Nucl. Chem. Art. 149 (1991) 109–118.
[17] X.H. Guan, J.S. Du, M. Xiaoguang, Y.K. Sun, B. Sun, Q.H. Hu, Application of titanium dioxide in arsenic removal from water: A review, J. Hazard. Mater 215–216 (2012) 1–16.
[18] G. Jegadeesan, S.R. Al-Abed, V. Sundaram, H. Choi, K.G. Scheckel, D.D. Dionysiou, Arsenic sorption on TiO_2 nanoparticles: Size and crystallinity effects, Water Res. 44 (2010) 965–973.
[19] H.Y. Niu, J.M. Wang, Y.L. Shi, Y.Q. Cai, F.S. Wei, Adsorption behavior of arsenic onto protonated titanate nanotubes prepared via hydrothermal method, Microporous Mesoporous Mater. 122 (2009) 28–35.
[20] M. Borho, P. Wilderer, Optimized removal of arsenate (III) by adaptation of oxidation and precipitation processes to the filtration step, Water Sci. Technol. 34 (1996) 25–31.
[21] C. Jing, X. Meng, E. Calvache, G. Jiang, Remediation of organic and inorganic arsenic contaminated groundwater using a nanocrystalline TiO_2-based adsorbent, Environ. Pollut. 157 (2009) 2514–2519.
[22] C. Gerente, V.K.C. Lee, P. Cloirec, G. McKay, Application of chitosan for the removal of metals from wastewaters by adsorption—Mechanisms and models review, Crit. Rev. Environ. Sci. Technol. 37 (2007) 41–127.
[23] M. Borho, P. Wilderer, Optimized removal of arsenate (III) by adaptation of oxidation and precipitation processes to the filtration step, Water Sci. Technol. 34 (1996) 25–31.
[24] X.H. Guan, J. Ma, H.R. Dong, L. Jiang, Removal of arsenic from water: Effect of calcium ions on As(III) removal in the KMnO4–Fe(II) process, Water Res. 43 (2009) 5119–5128.
[25] M. Bissen, M. Vieillard-Baron, A.J. Schindelin, F.H. Frimmel, TiO_2-catalyzed photooxidation of arsenite to arsenate in aqueous samples, Chemosphere 44 (2001) 751–757.
[26] H. Lee, W. Choi, Photocatalytic oxidation of arsenite in TiO_2 suspension: Kinetics and mechanisms, Environ. Sci. Technol. 36 (2002) 3872–3878.
[27] M.A. Ferguson, M.R. Hoffmann, J.G. Hering, TiO_2-photocatalyzed As (III) oxidation in aqueous suspensions: Reaction kinetics and effects of adsorption, Environ. Sci. Technol. 39 (2005) 1880–1886.
[28] G. Jegadeesan, S.R. Al-Abed, V. Sundaram, H. Choi, K.G. Scheckel, D.D. Dionysiou, Arsenic sorption on TiO_2 nanoparticles: Size and crystallinity effects, Water Res. 44 (2010) 965–973.
[29] H. Choi, Y.J. Kim, R.S. Varma, D.D. Dionysiou, Thermally stable nanocrystalline TiO_2 photocatalysts synthesized via sol–gel methods modified with ionic liquid and surfactant molecules, Chem. Mater. 18 (2006) 5377–5384.
[30] D.E. Tsydenov, A.A. Shutilov, G.A. Zenkovets, A.V. Vorontsov, Hydrous TiO_2 materials and their application for sorption of inorganic ions, Chem. Eng. J. 251 (2014) 131–137.
[31] T. Wajima, Y. Umeta, S. Narita, K. Sugawara, Adsorption behavior of fluoride ions using a titanium hydroxide-derived adsorbent, Desalination 249 (2009) 323–330.
[32] S.P. Suriyaraj, T. Vijayaraghavan, P. Biji, R. Selvakumar, Adsorption of fluoride from aqueous solution using different phases of microbially synthesized TiO_2 nanoparticles, J. Environ. Chem. Eng. 2 (2014) 444–454.
[33] S.S. Tripathy, S.B. Kanungo, Adsorption of Co^{2+}, Ni^{2+}, Cu^{2+} and Zn^{2+} from 0.5 M NaCl and major ion sea water on a mixture of δ-MnO_2 and amorphous FeOOH, J. Colloid Interface Sci. 284 (2005) 11–21.
[34] Y.Q. Zheng, E.W. Shi, Z.Z. Chen, W.J. Li, X.F. Hu, Influence of solution concentration on hydrothermal preparation of titania crystallites, J. Mater. Chem. 11 (5) (2001) 1547–1551.
[35] Y.Q. Zheng, E.W. Shi, W.J. Li, Z.Z. Chen, W.Z. Zhong, X.F. Hu, The formation of titania polymorphs under hydrothermal condition, Sci. China Ser. E 45(2) (2002) 120–129.
[36] N. Deedar, A. Irfan, Q. Ishtiaq, Evaluation of the adsorption potential of titanium dioxide nanoparticles for arsenic removal, J. Environ. Sci. 21 (2009) 402–408.
[37] P.K. Dutta, A.K. Ray, V.K. Sharma, F.J. Millero, Adsorption of arsenate and arsenite on titanium dioxide suspensions, J. Colloid Interface Sci. 278 (2004) 270–275.
[38] S.B. Deng, G. Yu, S.H. Xie, Q. Yu, J. Huang, Y. Kuwaki, M. Iseki, Enhanced adsorption of arsenate on the aminated fibers: Sorption behavior and uptake mechanism, Langmuir 24 (2008) 10961–10967.
[39] Y.S. Ho, G. McKay, Comparative sorption kinetic studies of dye and aromatic compounds onto fly ash, J. Environ. Sci. Health, A 34 (1999) 1179–1204.
[40] Z. Aksu, Equilibrium and kinetic modelling of cadmium(II) biosorption by *C. vulgaris* in a batch system: Effect of temperature, Sep. Purif. Technol. 21(3) (2001) 285–294.
[41] K.C. Justi, M.C.M. Laranjeira, A. Neves, A.S. Mangrich, V.T. Fávere, Chitosan functionalized with 2[-bis-(pyridylmethyl) aminomethyl]4-methyl-6-formyl-phenol: Equilibrium and kinetics of copper (II) adsorption, Polymer 45(18) (2004) 6285–6290.
[42] F.C. Wu, R.L. Tseng, R.S. Juang, Kinetic modeling of liquid-phase adsorption of reactive dyes and metal ions on chitosan, Water Res. 35(3) (2001) 613–618.
[43] R.H. Yao, F.P. Meng, L.J. Zhang, D.D. Ma, M.L. Wang, Defluoridation of water using neodymium-modified chitosan, J. Hazardous Mater. 165 (2009) 454–460.

[44] X.P. Liao, Y. Ding, B. Wang, B. Shi, Adsorption behavior of phosphate on metal-ions-loaded collagen fiber, Ind. Eng. Chem. Res. 45 (2006) 3896–3901.
[45] B. Kemer, D. Ozdes, A. Gundogdu, V.N. Bulut, C. Duran, M. Soylak, Removal of fluoride ions from aqueous solution by waste mud, J. Hazard. Mater. 168 (2009) 888–894.
[46] S. Kagne, S. Jagtap, P. Dhawade, S.P. Kamble, S. Devotta, S.S. Rayalu, Hydrated cement: A promising adsorbent for the removal of fluoride from aqueous solution, J. Colloid Interface Sci. 154 (2008) 88–95.
[47] Y. Ma, Y.M. Zheng, J.P. Chen, A zirconium based nanoparticle for significantly enhanced adsorption of arsenate: Synthesis, characterization and performance, J. Colloid Interface Sci. 354 (2011) 785–792.
[48] T.M. Suzuki, M.L. Tanco, D.A. Pacheco Tanaka, H. Matsunaga, T. Yokoyama, Adsorption characteristics and removal of oxo-anions of arsenic and selenium on the porous polymers loaded with monoclinic hydrous zirconium oxide, Sep. Sci. Technol. 36 (2001) 103–111.
[49] T.F. Lin, J.K. Wu, Adsorption of arsenite and arsenate within activated alumina grains: Equilibrium and kinetics, Water Res. 35 (2001) 2049–2057.
[50] K. Banerjee, G.L. Amy, M. Prevost, S. Nour, M. Jekel, P.M. Gallagher, C.D. Blumenschein, Kinetic and thermodynamic aspects of adsorption of arsenic onto granular ferric hydroxide (GFH), Water Res. 42 (2008) 3371–3378.
[51] Y.L. Tang, J.M. Wang, N.Y. Gao, Characteristics and model studies for fluoride and arsenic adsorption on goethite, J. Environ. Sci. 22 (2010) 1689–1694.
[52] R.Z. Chen, Z.Y. Zhang, Y.N. Yang, Z.F. Lei, N. Chen, X. Guo, Use of ferric-impregnated volcanic ash for arsenate (V) adsorption from contaminated water with various mineralization degrees, J. Colloid Interface Sci. 353 (2011) 542–548.
[53] R.Z. Chen, Z.Y. Zhang, C.P. Feng, K. Hu, M. Li, Y. Li, K. Shimizu, N. Chen, N. Sugiura, Application of simplex-centroid mixture design in developing and optimizing ceramic adsorbent for As(V) removal from water solution, Microporous Mesoporous Mater. 131 (2010) 115–121.
[54] B. Tatineni, M. Hideyuki, Adsorption characteristics of As(III) and As(V) with titanium dioxide loaded Amberlite XAD-7 resin, Anal. Sci. 18(12) (2002) 1345–1349.
[55] M.E. Pena, G.P. Korfiatis, M. Patel, L. Lippincott, X.G. Meng, Adsorption of As(V) and As(III) by nanocrystalline titanium dioxide, Water Res. 39 (2005) 2327–2337.
[56] P.K. Dutta, A.K. Ray, V.K. Sharma, F.J. Millero, Adsorption of arsenate and arsenite on titanium dioxide suspensions, J. Colloid. Interface Sci. 278 (2004) 270–275.
[57] M. Pirilä, M. Martikainen, K. Ainassaari, T. Kuokkanen, R.L. Keiski, Removal of aqueous As(III) and As(V) by hydrous titanium dioxide, J. Colloid Interface Sci. 353 (2011) 257–262.
[58] S. Bang, M. Patel, L. Lippincott, X.G. Meng, Removal of arsenic from groundwater by granular titanium dioxide adsorbent, Chemosphere 60 (2005) 389–397.
[59] G.S. Zhang, J.H. Qu, H.J. Liu, R.P. Liu, R.C. Wu, Preparation and evaluation of a novel Fe–Mn binary oxide adsorbent for effective arsenite removal, Water Res. 41 (2007) 1921–1928.
[60] S.B. Deng, Z.J. Li, J. Huang, G. Yu, Preparation, characterization and application of a Ce–Ti oxide adsorbent for enhanced removal of arsenate from water, J. Hazard Mater. 179 (2010) 1014–1021.
[61] C.-K. Na, H.-J. Park, Defluoridation from aqueous solution by lanthanum hydroxide, J. Hazard. Mater. 183 (2010) 512–520.
[62] A.A.M. Daifullah, S.M. Yakout, S.A. Elreefy, Adsorption of fluoride in aqueous solutions using $KMnO_4$-modified activated carbon derived from steam pyrolysis of rice straw, J. Hazard. Mater. 147 (2007) 633–643.
[63] N.A. Medellin-Castillo, R. Leyva-Ramos, R. Ocampo-Perez, R.F. Garcia de la Cruz, A. Aragon-Piña, J.M. Martinez-Rosales, R.M. Guerrero-Coronado, L. Fuentes-Rubio, Adsorption of fluoride from water solution on bone char, Ind. Eng. Chem. Res. 46 (2007) 9205–9212.
[64] E. Kumar, A. Bhatnagar, M. Ji, W. Jung, S.H. Lee, S.J. Kim, G. Lee, H. Song, J.Y. Choi, J.S. Yang, B.H. Jeon, Defluoridation from aqueous solutions by granular ferric hydroxide (GFH), Water Res. 43 (2009) 490–498.
[65] E. Tchomgui-Kamga, V. Alonzo, C.P. Nanseu-Njiki, N. Audebrand, E. Ngameni, A. Darchen, Preparation and characterization of charcoals that contain dispersed aluminum oxide as adsorbents for removal of fluoride from drinking water, Carbon 48 (2010) 333–343.
[66] N. Das, P. Pattanaik, R. Das, Defluoridation of drinking water using activated titanium rich bauxite, J. Colloid Interface Sci. 292 (2005) 1–10.
[67] L. Chen, B.Y. He, S. He, T.J. Wang, C.L. Su, Y. Jin, Fe–Ti oxide nano-adsorbent synthesized by co-precipitation for fluoride removal from drinking water and its adsorption mechanism, Powder Technol. 227 (2012) 3–8.
[68] Z.J. Li, S.B. Deng, X.Y. Zhang, W. Zhou, J. Huang, G. Yu, Removal of fluoride from water using titanium-based adsorbents, Front. Environ. Sci. Eng. Chin. 4 (2010) 414–420.
[69] K. Biswas, D. Bandhoyapadhyay, U.C. Ghosh, Adsorption kinetics of fluoride on iron(III)-zirconium(IV) hybrid oxide, Adsorption 13 (2007) 83–94.
[70] M.S. Onyango, Y. Kojima, O. Aoyi, E.C. Bernardo, H. Matsuda, Adsorption equilibrium modeling and solution chemistry dependence of fluoride removal from water by trivalent-cation-exchanged zeolite F-9, J. Colloid Interface Sci. 279 (2004) 341–350.
[71] H. Genç, J.C. Tjell, D. McConchie, O. Schuiling, Adsorption of arsenate from water using neutralized red mud, J. Colloid Interface Sci. 264(2) (2003) 327–334.
[72] K. Gupta, U.C. Ghosh, Arsenic removal using hydrous nanostructure iron(III)–titanium(IV) binary mixed oxide from aqueous solution, J. Hazard. Mater. 161 (2009) 884–892.